Comparative Analysis of Five Standard Dry Tropospheric Delay Models for Estimation of Dry Tropospheric Delay in Gnss Positioning

Opaluwa Y. D, Adejare Q. A[*], Suleyman Z. A. T, Abazu I. C,

Adewale T. O, Odesanmi A. O, Okorocha V. C

Department of Surveying & Geoinformatics, Federal University of Technology, Minna, Niger State, Nigeria

Abstract   The atmosphere causing the delay in GPS signals consists of two main layers, ionosphere and troposphere. The ionospheric bias can be mitigated using dual frequency receivers. Unlike the ionospheric bias, the tropospheric bias cannot be removed using the same procedure. Compensation for the tropospheric bias is often carried out using a standard tropospheric model. In order to investigate the impact of different dry tropospheric models on GPS accuracy, simultaneous hourly observations was carried out at some selected stations in Minna. The tropospheric errors obtained using five standard tropospheric models namely, the Saastamoinen model (which was adopted as the standard model), Hopfield model, Davis et al. model, Saastamoinen model (Using Ground Meteorological Data) and Altshuler and Kalaghan model were compared. It was deduced from the results that at all the stations, the Saastamoinen Model (Using Ground Meteorological Data), has 100% correlation with the adopted standard Dry Tropospheric Model (Saastamoinen model). While a standard error of 0.285mm, 1.446mm and 2.899mm were respectively obtained for Davis et al. Model, Hopefield model and Altshuler and Kalaghan (A&K) Model. However, the statistical test performed on the overall results indicated that there is no significant difference in the performance of the five tropospheric models at 0.05 significance level. It was therefore, concluded that either of the five models evaluated in this study can perform well in the study area, nevertheless, the choice of Saastamoinen Model, Saastamoinen Model (Ground Meteorological Data) and Davis et al. Model will be more preferable.

Keywords   Ionospheric Bias, Troposheric Bias, GPS Signal, Tropospheric Models

1. Introduction

1.1. Background to Study

The propagation delay induced by the electrically neutral atmosphere, commonly known as the tropospheric delay, is one of the most difficult-to-model errors affecting space geodetic techniques. An unmodelled tropospheric delay affects mainly the height component of position and therefore constitutes a matter of concern in space-geodesy applications, such as sea-level monitoring, post-glacial rebound measurement, earthquake-hazard mitigation, and tectonic-plate-margin deformation studies, where the highest possible position accuracy is sought, hence the improvement in tropospheric delay modelling is therefore essential[19].

When travelling through the electrically-neutral atmosphere, radio signals used by radiometric techniques are affected by the variability of the refractive index, causing an excess path delay and ray bending. The effect is commonly known as tropospheric propagation delay (or simply tropospheric delay), even though this designation is misleading, as the stratosphere has a significant contribution to the total delay[8]. The troposphere is an effectively non-dispersive region up to frequencies of approximately 15GHz for microwave signals. In other words the propagation through the troposphere is not frequency dependent.

The delay caused by the troposphere can be separated into two main components: the hydrostatic delay and the wet delay [13]. The zenith hydrostatic delay (dry component) contributes about 90% of the total delay to the tropospheric delay[16]. The dry component is determined with high accuracy by many tropospheric delay models derived from surface measurements. Since the dry part of the troposphere is in hydrostatic equilibrium, the ideal gas law can easily be applied to it. The wet component, however, is difficult to predict because of the irregular distribution of liquid water and water vapour both horizontally and vertically in the troposphere. Although the wet component of the delay constitutes less than 10% of the total effect[9], it still causes the limiting uncertainty in determining a very accurate remedy for the total delay. The tropospheric delay is difficult to fully correct and constitutes one of the major

* Corresponding author:
quadriadejare@yahoo.com (Adejare Q. A)

residual error sources in modern space geodetic techniques such as–DORIS (Doppler Orbitography and Radio-positioning Integrated by Satellite), GPS (Global Positioning System) and VLBI (Very Long Baseline Interferometry) – affecting mainly the estimates of the height component of position[16].

1.2. Statement of Problem

Tropospheric delay is one of the major errors in Global Navigation Satellite System (GNSS) Positioning. Several models exist for estimating the magnitude of this error in the determined positions, but the level of refinement attainable with each of the models differs. Furthermore, the effect of tropospheric delay has been accounted for in dual frequency GPS receivers, but the impact is still significant in single frequency receivers. Since most GNSS users in the study area cannot easily afford dual frequency receiver, there is the need to assess the performance of some standard tropospheric models in the area. Therefore, this research seeks to compare some dry tropospheric delay models in Minna using data observed with single frequency Differential GPS (DGPS).

1.3. Aim and Objectives

The aim of this research is to identify the optimum dry tropospheric model using single frequency GPS receivers. Therefore, the objectives that will assist in achieving the above aim include the following:

- To carry out DGPS observations at three (3) epochs of the day (i.e. morning, afternoon and evening), as well as atmospheric parameters such as temperature, relative humidity, pressure, etc at some selected stations in Minna.

- To estimate the amount of dry tropospheric delay with each model at various epochs of observation using a program written in Java programming language.

- To examine the differences in the estimated delay using the selected models and perform statistical tests on the results.
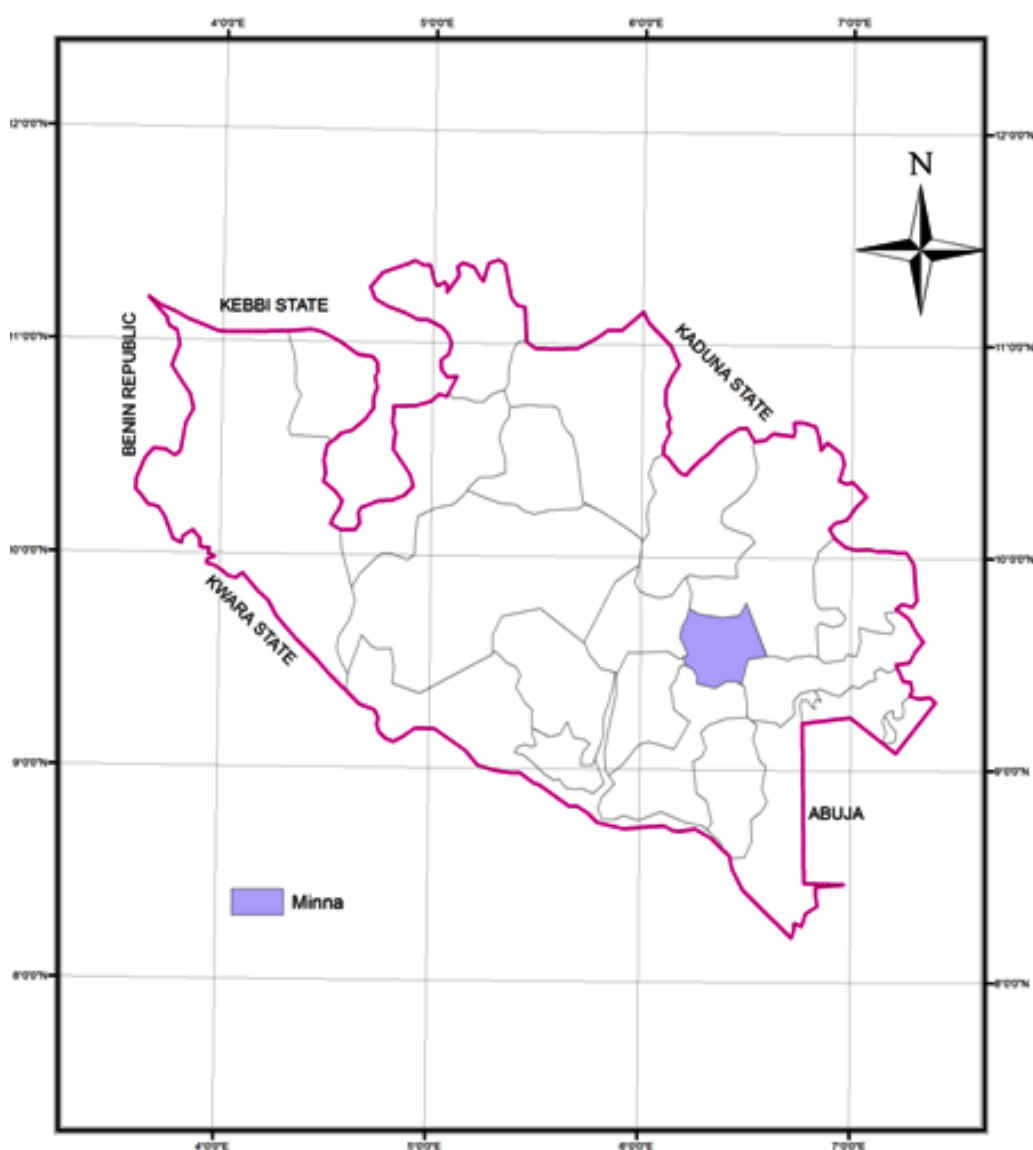

Figure 1(a).   Administrative Map of Niger State showing Minna. (Source: Niger State Ministry of Lands)
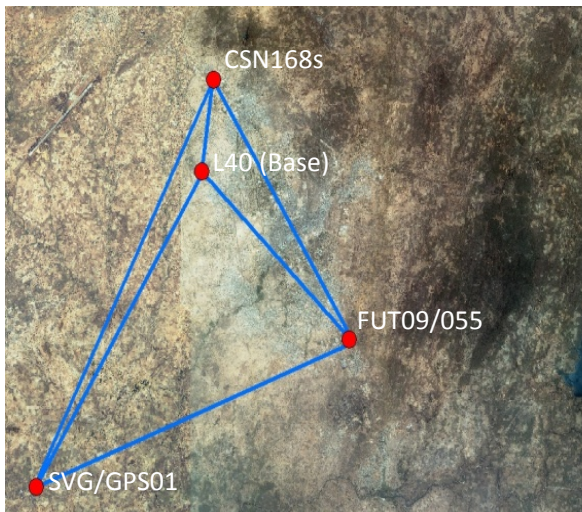
Figure 1(b).   Observed stations for the study

1.4. Location and Scope of Study

1.4.1. Location of Project

The project site was located in Minna, the capital of Niger state. The city is with an estimated population of over 347,788 and land area of about 6.784 square kilometres. Minna lies between latitudes $9^030'00''$ and $11^030'00''$ North of the Equator and longitudes $6^030'00''$ and $7^030'00''$ East of the Meridian, on a geological base of copper, iron, lead, silica, clay, sand, etc (Niger State Diary, 2010). The stations were carefully selected to cover the major axes of Minna, as they are located at House of Assembly Quarters (09/FUT/055), Tudun Fulani (CSN168s), Gidan-Kwano campus of Federal University of Technology Minna (SVG/GPS/01/2008), and at Minna-L40 datum. Figure 1 shows the map of the study area, with the stations in red.

1.4.2. Scope of Project

The scope of this project covers data collection using DGPS (Differential GPS) technique and the estimation of dry tropospheric delay in the data using appropriate models computed with a Java Program. This project does not cater for the wet tropospheric component and other error sources in GPS observation.

2. Conceptual Framework

2.1. Differential Global Positioning System (DGPS)

The DGPS is an enhancement to Global Positioning System that uses a network of fixed, ground-based reference stations to broadcast the difference between the positions indicated by the satellite systems and the known fixed positions. These stations broadcast the difference between the measured satellite pseudoranges and actual (internally computed) pseudoranges, and receiver stations may correct their pseudoranges by the same amount. The correction signal is typically broadcast over

UHF radio modem[11]. DGPS data collection can be by static, stop-and-go, and kinematics modes. The three modes run independently. In the *Static* data collection mode, the GPS receiver systems simultaneously collect raw data from all available satellites while remaining stationary on their respective points. In the *Stop-and-Go* data collection mode, the GPS receiver systems simultaneously collect raw data from all available satellites while stationary on their respective points and while moving between points. In the *Kinematics* data collection mode, the GPS receiver systems simultaneously collect raw data from all available satellites while a receiver is moving[10] about 100km above it. The lower part of this shell, ranging from the surface of the Earth to approximately 50km above it, contains about 99.9% of all atmospheric mass. It consists of the troposphere (0-10km), in which temperature decreases with height, the tropopause (10km), at which temperature remains constant, and the stratosphere (10-50km), in which temperature increases with height. The delay experienced by a signal travelling through the neutral part of atmosphere is generally referred to as tropospheric delay, since the troposphere accounts for 90% of the total delay. Therefore, when speaking of the troposphere, often the lower 50km of the Earth's atmosphere is really referred to[8].
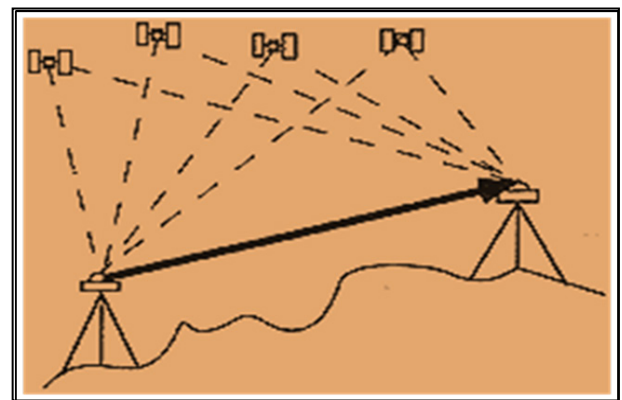

Figure 2.   Principle of DGPS Observation

2.2. Troposphere

The neutral (non-ionized) atmosphere is an approximately spherical shell extending outward from the Earth's surface to The tropospheric effect is a further factor elongating the runtime of electromagnetic waves by refraction. The reasons for the refraction are different concentrations of water vapour in the troposphere, caused by different weather conditions. The error cannot be eliminated by calculation. It can only be approximated by a general calculation model[16]. The tropospheric delay is separated into two components: dry and wet. The dry component is determined with high accuracy by many tropospheric delay models derived from surface measurements. The wet component, however, is difficult to predict because water vapour is highly variable in space and time such that the wet delay cannot be modelled using surface measurements very accurately[1]. The wet component of the delay constitutes less than 10% of the total effect; tropospheric effect on GPS signals is approximately ± 0.5m[8]. Figure 3

shows the various layers of the atmosphere and the response of air temperature to increasing altitude.

2.2.1. Hydrostatic Models

Early efforts to determine corrections for radio propagation delay by the atmosphere were prompted by the need for improvements in satellite tracking from ground stations.
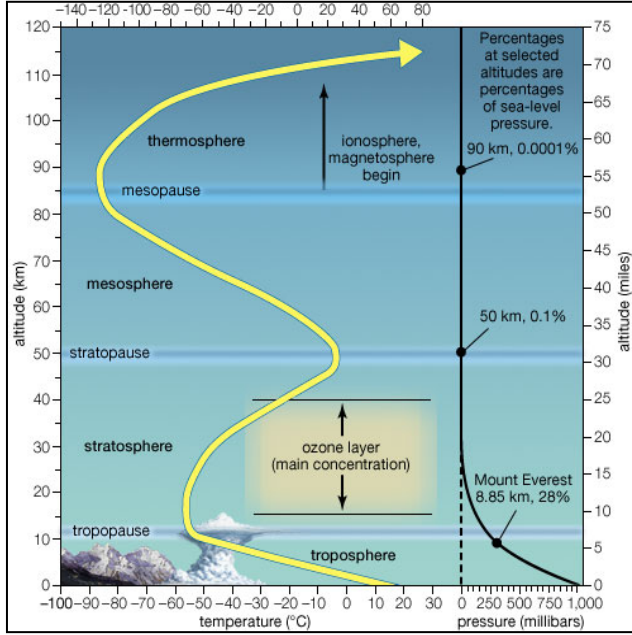

Figure 3. The Layers of Earth's Atmosphere. Source:[5]

[13],[12], and[2] made significant contributions to the study of range corrections. Saastamoinen's Zenith hydrostatic delay and the form of Marini's approximation for the mapping function for a horizontally stratified refractive medium are incorporated in many current models used for accurate space-based geodetic measurements.

[13] Showed that the delay in the zenith direction due to the atmospheric constituents in hydrostatic equilibrium is accurately determined by measuring the surface pressure and making corrections for the latitude and height above sea level of the site from which the observation was made. His formula (or slightly more precise form given by[3] provides the zenith hydrostatic path with accuracy better than 1mm under conditions of hydrostatic equilibrium.

[15] investigated the impact of different standard tropospheric models (namely, Saastamoinen model, Hopfield model and Simplified Hopfield model) on GPS baseline accuracy, in order to determine the best-fit standard tropospheric model in Thailand with the GPS data collected in Thailand.

The results indicated that there are no statistically significant differences in the performance of the three tropospheric models. However, the use of the Saastamoinen model tends to produce more reliable results than the use of the other two models[15].

(i). Saastamoinen Model

If hydrostatic equilibrium is assumed, the hydrostatic delay model may be expressed simply as a function of measured surface pressure.[14] employed this approach and used the following representation of gravity g_m in the zenith hydrostatic model.

$$g_m = 9.784(1 - 0.0026\cos 2\varphi - 0.00000028 H_s) \quad (1)$$

Where, φ is the latitude of the station and H_s is the station height above sea level, in metres. Saastamoinen used K_1 refractivity constant given by[3] to determine the following expression for the zenith hydrostatic delay:

$$d_h^z = \frac{0.002277 P_s}{(1 - 0.0026\cos 2\varphi - 0.00000028 H_s)} \quad (2)$$

where, P_s is the surface pressure and $K_1 = 0.0022768$.

The most stable tropospheric model for the equatorial region is the Saastamoinen Model[15]. Consequently, Saastamoinen Model has been adopted as the Standard dry Tropospheric delay Model for this research.

(ii). Davis et al. Model

The[4] model slightly differs from the Saastamoinen model. Davis el al. used the K_1 refractivity constant given by[20] and the zenith hydrostatic model is given by the following expression:

$$d_h^z = \frac{0.0022768 P_s}{(1 - 0.0026\cos 2\varphi - 0.00000028 H_s)} \quad (3)$$

where, P_s is the surface pressure and $K_1 = 0.0022768$.

(iii). Hopfield Model

[7] assumed that the theoretical dry refractivity profile could be expressed using a quartic model:

$$N_d = N_{ds} \frac{(H_d^e - H)^4}{(H_d^e)^4} \quad (4)$$

where, $H_d^e = 40136 + 148.72(T - 273.16)$, N_{ds} is the dry refractivity on the surface obtained using the K_2 refractivity constant determined by[17] as $77.6 \times 10^{-6} \frac{P_s}{T_s}$ and H is the height above sea level, in metres hence, the final expression for the zenith dry delay can be represented by the following expression:

$$d_d^z = 77.6 \times 10^{-6} \frac{P_s}{T_s} \frac{H_d^e}{S} \quad (4.1)$$

where, P_s is the surface pressure, and T_s is the surface temperature and K_2 is 2.29286.

(iv). Altshuler and Kalaghan (A&K) Model

Using the K_2 refractivity constant determined by[17], the tropospheric delay correction (Δ) in metres is given by[18]:

$$\Delta(E, h, N_s) = 0.3048 \times 2.29286 \times m(E) \times H(h) \times F(h, N_s) metres \quad (5)$$

where,

$$m(E) = \frac{1}{2.29286}\left\{\begin{array}{l}(0.1556 + \frac{138.8926}{E} - \frac{105.0574}{E^2} + \frac{31.507}{E^2}) + \\ [1.0 + 10^{-4}(E - 30)^2]\end{array}\right\} \quad (5.1)$$

$$H(h) = 0.0097 - \frac{2.08809}{h+8.6286} + \frac{122.73592}{(h+8.6286)^2} - \frac{703.82166}{(h+8.6286)^2} \quad (5.2)$$

$$F(h,N_s) = 3.28084 \left(\begin{array}{c} \frac{6.81758}{h+3.28084} + 0.3048(h+3.28084) + \\ 0.00423N_s - 1.33333 \end{array} \right) \quad (5.3)$$

$$(1 - 1.41723 \times 10^{-6}(N_s - 315))$$

$$N_s = 77.604 \left(\frac{P_s}{T_s} \right)$$

E = elevation angle in degrees

h = height above sea level in metres

N_S = global surface refractivity

P_s = surface pressure in milibars

T_s = surface temperature in degree Kelvin

K_2 = 2.29286m

(v). Saastamoinen Model (Using Ground Meteorological Data)

Using the K_1 refractivity constant determined by[4], the tropospheric delay using this model is given by[18]:

$$d_h^z = \frac{0.0022767P}{(1 - 0.00266\cos 2\varphi - 0.00000028H)} \quad (6)$$

where, P_s is the atmospheric pressure, φ is the latitude of the station and H is the height of the station above sea level, K1 is 0.002277 in metres.

3. Methodology

During planning, the stations were carefully selected to cover the major axes of Minna using the city map of Minna. The stations are 09/FUT/055 at House of Assembly Quarters, CSN168S at Tudun Fulani, SVG/GPS/01/2008 at Gidan-Kwano campus of Federal University of Technology Minna, and L40 Nigerian datum (base station) see fig. 1 above. The coordinates of the selected stations were collected from the Department of Surveying & Geoinformatics, Federal University of Technology Minna. The details are as shown in the table below:

Table 1. Existing Coordinates of Stations Used

STATIONS	NORTHINGS (m)	EASTINGS (m)	HEIGHT (m)
L40	1066041.870	227423.232	279.603
CSN168S	1069224.788	227914.615	306.646
FUT 09/055	1060188.295	233413.820	268.390
SVG/GPS/01	1055093.618	220563.650	234.138

3.1. Data Acquisition Procedure

Thales ProMark3 Single Frequency DGPS Receivers and the Accessories were used. The static DGPS procedure was used for the field operation. The instrument was set at Minna-L40 datum, which was adopted as the base station. All necessary adjustments were carried out before the necessary parameters

were entered into the receiver to start observations. The other three stations were similarly set up and were simultaneously log on to capture data concurrently for an hour, four sets of hourly observation was made during each session.

This simultaneous observations were made at all stations between 8:30a.m and 12 noon for morning observation, 2:00p.m and 5:00p.m for afternoon observation, 6:00p.m and 9:00p.m for evening observation.
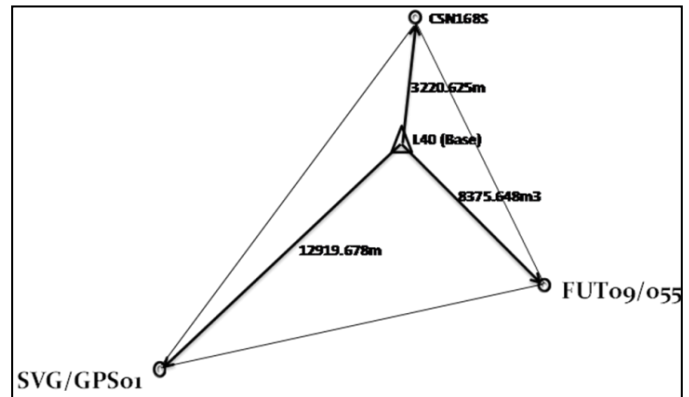

Figure 4. Network design

3.2. Data Processing

Since the ProMark3 System operates in conjunction with GNSS Solutions, the acquired field data were processed using GNSS solutions Software. Also, a Java 1.6.0_15 based Program was developed using the selected dry tropospheric delay models. The Java program runs with an installed My SQL Administrator (version 1.1.9) and Net Beans IDE (6.5). The equations defining the models were coded into the program with SQL for fast, efficient and error-free processing to obtain the tropospheric delay.

4. Results and Analysis

4.1. Results

Below are the mean coordinates obtained from the field observations.

Table 2(a). Coordinates of Occupied Stations during Morning Observations

Point ID	Easting(m)	Northing(m)	Height(m)
L40	227423.232	1066041.870	279.603
FUTO9/055	233413.977	1060188.317	268.620
GPS01	220563.610	1055093.227	238.305
CSN168s	227913.915	1069224.587	307.922

Table 2(b). Coordinates of Occupied Stations during Afternoon Observations

Point ID	Easting(m)	Northing(m)	Height(m)
L40	227423.232	1066041.870	279.603
FUT09/055	233413.995	1060188.311	268.673
GPS 01	220563.586	1055093.221	238.245
CSN168s	227913.925	1069224.574	308.025

Table 2(c).   Coordinates of Occupied Stations during Evening Observations

Point ID	Easting(m)	Northing(m)	Height(m)
L40	227423.232	1066041.870	279.603
FUT09/055	233414.011	1060188.315	268.694
GPSS01	220563.760	1055093.165	238.262
CSN168s	227913.901	1069224.557	308.020

Tables 2(a, b, c) above show the processed three–dimensional (X, Y, Z) coordinates of the occupied stations during morning, afternoon and evening observations using GNSS Solutions.

Tropospheric delay affects mainly the height components [19]. Hence, table 3 below shows the mean observed heights at the various occupied stations during observations.

Table 3.   Summary of Observed Heights

Statn	Epoch	L 40	FUT 09/055	SVG/ GPS01	CSN 168S
Observed Heights (m)	Morning	279.603	268.621	238.305	307.920
	Afternoon	279.603	268.673	238.245	308.025
	Evening	279.603	268.694	238.262	308.020
	Mean of Means	279.603	268.663	238.271	307.988

Tables 4 (a to E) below show the dry tropospheric errors estimated by the different tropospheric models during morning, afternoon and evening observations.

Tables 5, 6, 7, 8 below show the deviations of the tropospheric delay estimated by the other dry tropospheric models from the adopted standard model (Saastamoinen model) at each station.

♦ KEY:

M_1: SAASTAMOINEN Model, M_2: SAASTAMOINEN Model (GROUND MET. DATA),

M_3: DAVIS, M_4: Altshuler and Kalaghan (A&K) Model and M_5: HOPFIELD Model

♦ NOTE: Standard Model adopted is Saastamoinen Dry Tropospheric Model[15].

Chart 1 below shows graphically, the deviations of tropospheric error estimated by other tropospheric delay models at L – 40 datum in the above table.

The Chart 2 below shows graphically, the deviations of tropospheric error estimated by other tropospheric delay models at FUT09/055 station in the above table.

The Chart 3 below shows graphically, the deviations of tropospheric error estimated by other tropospheric delay models at SVG/GPS01 station in the above table.

The Chart 4 below shows graphically, the deviations of tropospheric error estimated by other tropospheric delay models at CSN168s station in the above table.

Table 4.   Dry Tropospheric Error Estimates by Each Model per station

STATION EPOCH	L40	FUT09/ 055	SVG/ GPS 01	CSN 168s
A. SAASTAMOINEN MODEL				
Morning	2.25103	2.25102	2.251	2.25105
Afternoon	2.24699	2.24699	2.24697	2.24701
Evening	2.24768	2.24767	2.24765	2.24769
MEAN ESTIMATE	**2.248567**	**2.24856**	**2.24854**	**2.248583**
B. SAASTAMOINEN (GROUND MET. DATA) MODEL				
Morning	2.25103	2.25102	2.251	2.25105
Afternoon	2.24699	2.24699	2.24697	2.24701
Evening	2.24768	2.24767	2.24765	2.24769
MEAN ESTIMATE	**2.248567**	**2.24856**	**2.24854**	**2.248583**
C. DAVIS ET. AL MODEL				
Morning	2.25083	2.25083	2.25081	2.25085
Afternoon	2.24509	2.24679	2.24677	2.24681
Evening	2.24748	2.24747	2.24745	2.24750
MEAN ESTIMATE	**2.2478**	**2.248363**	**2.248343**	**2.248387**
D. ALTSHULER AND KALAGHAN (A&K) MODEL				
Morning	0.02244	0.02137	0.01812	0.0252
Afternoon	0.02052	0.0204	0.018	0.02519
Evening	0.02295	0.02186	0.01854	0.02557
MEAN ESTIMATE	**0.02197**	**0.02121**	**0.01822**	**0.02532**
E. HOPFIELD MODEL				
STATION⇒ EPOCH ⇓	L40	FUT09/ 055	SVG/ GPS 01	CSN 168s
Morning	0.01427	0.01371	0.01216	0.01572
Afternoon	0.01413	0.0136	0.01204	0.01556
Evening	0.0142	0.01365	0.0121	0.01565
MEAN ESTIMATE	**0.0142**	**0.013653**	**0.0121**	**0.015643**

Table 5.   Deviation of Other Models from the Standard Dry Tropospheric Model at L-40

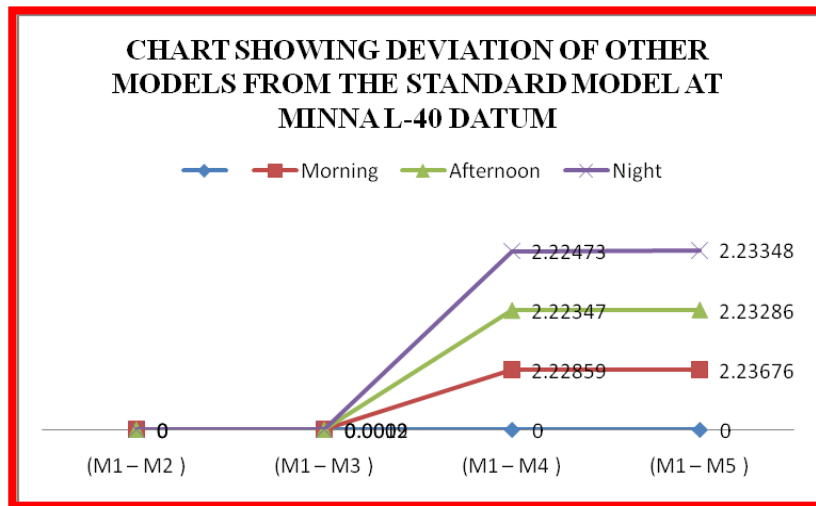| Diff	Epoch	$(M_1 - M_2)$	$(M_1 - M_3)$	$(M_1 - M_4)$	$(M_1 - M_5)$
Dry Tropospheric Errors	Morning	0.00000	0.00020	2.22859	2.23676
	Afternoon	0.00000	0.00190	2.22347	2.23286
	Evening	0.00000	0.00020	2.22473	2.23348
	Mean	0.00000	0.00767	2.22560	2.23437

Chart 1. Deviation of Other Models from the Standard Model at L-40

Table 6. Deviation of Other Models from the Standard Dry Troposheric Model at FUT09/055

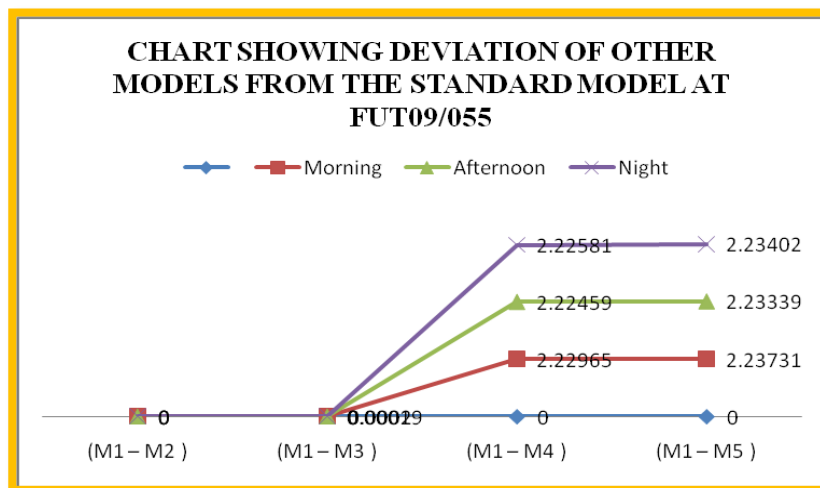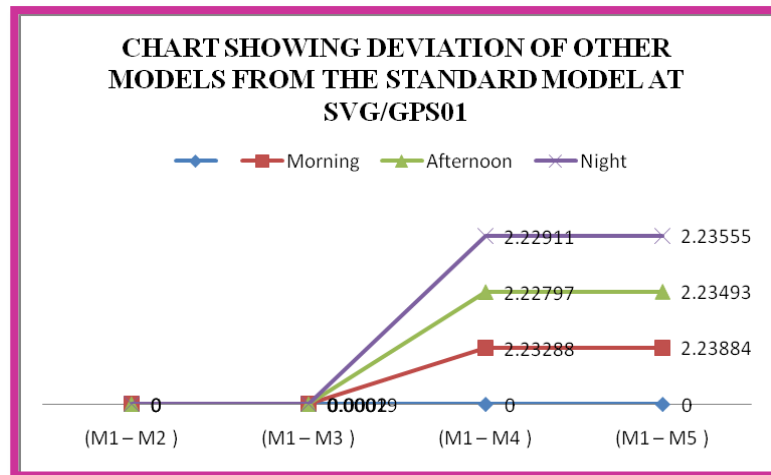| Diff	Epoch	$(M_1 - M_2)$	$(M_1 - M_3)$	$(M_1 - M_4)$	$(M_1 - M_5)$
Dry Tropospheric Errors	Morning	0.00000	0.00019	2.22965	2.23731
	Afternoon	0.00000	0.00000	2.22459	2.23339
	Evening	0.00000	0.00020	2.22581	2.23402
	Mean	0.00000	0.00013	2.22668	2.23491

Chart 2. Deviation of Other Models from the Standard Model at FUT09/055

Table 7. Deviation of Other Models from the Standard Dry Troposheric Model at SVG/GPS01

Diff	Epoch	$(M_1 - M_2)$	$(M_1 - M_3)$	$(M_1 - M_4)$	$(M_1 - M_5)$
Dry Tropospheric Errors	Morning	0.00000	0.00019	2.23288	2.23884
	Afternoon	0.00000	0.00020	2.22797	2.23493
	Evening	0.00000	0.00020	2.22911	2.23555
	Mean	0.00000	0.00197	2.23000	2.23644

Chart 3.   Deviation of Other Models from the Standard Model at SVG/GPS01
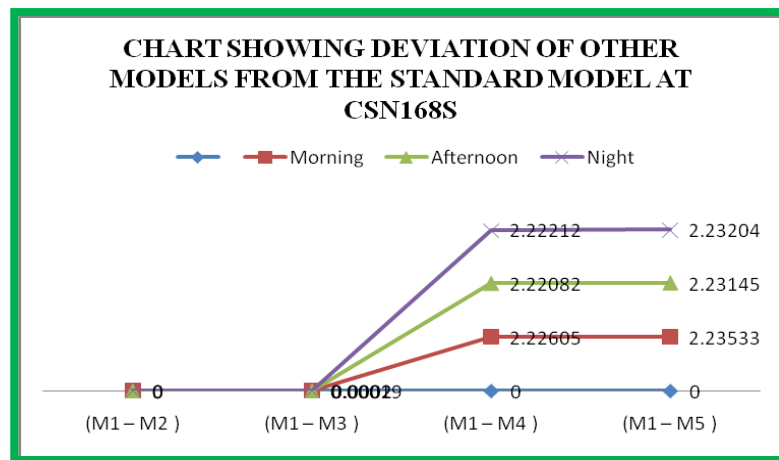

Chart 4.   Deviation of Other Models from the Standard Model at CSN168S

Table 8.   Deviation of Other Models from the Standard Dry Troposheric Model at CSN168S

Diff	**Epochs**	$(M_1 - M_2)$	$(M_1 - M_3)$	$(M_1 - M_4)$	$(M_1 - M_5)$
Dry Tropospheric Errors	Morning	0.00000	0.00020	2.22605	2.23533
	Afternoon	0.00000	0.00020	2.22082	2.23145
	Evening	0.00000	0.00019	2.22212	2.23204
	Mean	0.00000	0.00197	2.22300	2.23294

Table 9.   Mean Estimate of tropospheric error per station per model

Statn	Saastam.	Saas. Grnd Met	Davis et al.	Altsh & Kalaghn	Hope Field
L40	2.2485667	2.248567	2.2478	0.02197	0.0142
FUT09/055	2.24856	2.24856	2.248363	0.02121	0.01365
SVG/GPS01	2.24854	2.24854	2.248343	0.01822	0.0121
CSN 168S	2.2485833	2.248583	2.248387	0.02532	0.01564

Table 10.   Mean deviation per station per model

Statn	Saas. Grnd Met	Davis et al.	Altsh & Kalaghn	Hope Field
L40	0.0000	0.000767	2.226597	2.234367
FUT09/055	0.0000	0.000197	2.22735	2.234907
SVG/GPS01	0.0000	0.000197	2.23032	2.23644
CSN168S	0.0000	0.000197	2.223263	2.23294

In a further investigation, the hypothesis test was carried out to find out if the differences in the performance of the five (5) standard tropospheric Models at each station are statistically significant at 5% significance level using **StatextV1.0** software.

The hypothesis is as follows:

H$_0$: μ$_1$ = μ$_2$ = μ$_3$ (Null hypothesis)

H$_1$: at least two are not equal (Alternative hypothesis)

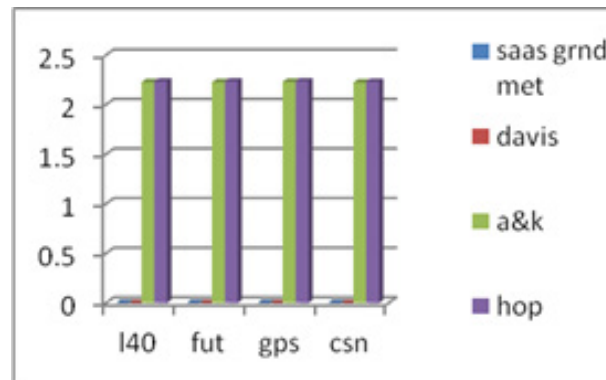Reject F, if F$_{0.95}$ > F-Table, otherwise accept null hypothesis.

Chart 5. Mean deviation

Table 11. Test of Significant Difference between Saastamoinen Model & Davis et al. Model

Statn	Epoch	Saastamoinen	Davis	F$_{0.95}$ (1,4) Ratio	F$_{0.95}$ (1,4) Table	Rem
L 40	Morning	2.25103	2.25083	0.140	F(1,4) = 7.71	Accept
	Afternoon	2.24699	2.24509			
	Evening	2.24768	2.24748			
FUT09/055	Morning	2.25102	2.25083	0.010	F(1,4) = 7.71	Accept
	Afternoon	2.24699	2.24699			
	Evening	2.24767	2.24747			
SVG/ GPS01	Morning	2.25100	2.25081	0.010	F(1,4) = 7.71	Accept
	Afternoon	2.24697	2.24677			
	Evening	2.24765	2.24745			
CSN 168S	Morning	2.25105	2.25085	0.010	F(1,4) = 7.71	Accept
	Afternoon	2.24701	2.24681			
	Evening	2.24769	2.24750			

Table 12. Test of Significant Difference between Saastamoinen Model & Altshuler & Kalaghan (A & K) Model

Statn	Epoch	Saastamoinen	A & K	F$_{0.95}$(1,4) Ratio	F$_{0.95}$ (1,4) Table	Rem
L40	Morning	2.25103	0.02244	0.490	F(1,4) = 7.71	Accept
	Afternoon	2.24699	0.02352			
	Evening	2.24768	0.02295			
FUT09/055	Morning	2.25102	0.02137	0.960	F(1,4) = 7.71	Accept
	Afternoon	2.24699	0.02240			
	Evening	2.24767	0.02186			
SVG/GPS01	Morning	2.25100	0.01812	0.650	F(1,4) = 7.71	Accept
	Afternoon	2.24697	0.01900			
	Evening	2.24765	0.01854			
CSN 168S	Morning	2.25105	0.02500	0.090	F(1,4) = 7.71	Accept
	Afternoon	2.24701	0.02619			
	Evening	2.24769	0.02557			

Table 13. Test of Significant Difference between Saastamoinen Model & Hopfield Model

Statn	Epoch	Saastamoinen	Hope-field	$F_{0.95}(1,4)$ Ratio	$F_{0.95}(1,4)$ Table	Rem
L40	Morning	2.25103	0.01427			
	Afternoon	2.24699	0.01413	0.240	F(1,4) = 7.71	Accept
	Evening	2.24768	0.01420			
FUT 09/055	Morning	2.25102	0.01371			
	Afternoon	2.24699	0.01360	0.640	F(1,4) = 7.71	Accept
	Evening	2.24767	0.01365			
SVG GPS01	Morning	2.25100	0.01216			
	Afternoon	2.24697	0.01204	0.990	F(1,4) = 7.71	Accept
	Evening	2.24765	0.01210			
CSN 168S	Morning	2.25105	0.01572			
	Afternoon	2.24701	0.01556	0.410	F(1,4) = 7.71	Accept
	Evening	2.24769	0.01565			

4.2. Analyses of Results

In the following analyses, the discrepancies in the dry tropospheric errors obtained by the five tropospheric models at various observation epochs are discussed. It can be seen from Tables 2, 3 and 4 above showed that Hopfield Model has the lowest dry tropospheric delay estimates numerically while the highest dry tropospheric estimates are from Saastamoinen and Saastamoinen (Using Ground Meteorological Data) Models. The performance of Saastamoinen, Saastamoinen (Using Ground Meteorological Data) and Davis et al. standard tropospheric Models are very close as their dry tropospheric errors differ only by a few centimetres during morning, afternoon and evening observations, while Altshuler and Kalaghan (A&K) Model and Hopfield Model have centimetre variations among each other but differ from the other three by about two metres (2m).

The reason for this is that Saastamoinen, Saastamoinen et al. standard tropospheric Models used the same empirically determined refractivity constant (k_1), while Altshuler and Kalaghan (A&K) Model and Hopfield Model used the same empirically determined refractivity constant (k_2). Also, it can be seen that there are no variations in the dry tropospheric errors estimated by Saastamoinen Model and Saastamoinen Model (Using Ground Meteorological Data) during morning, afternoon and evening observations.

Tables 5, 6, 7, 8 and Charts 1, 2, 3, 4 depicted the absolute deviations of the dry tropospheric Models from Saastamoinen Model which was adopted as the standard Model [15] at each station. This gave the idea of the temporal variability of the estimated tropospheric error by the models. Since Saastamoinen Model (Using Ground Meteorological Data) is highly correlated with the adopted standard model because of the model similarity, the remaining three models were evaluated. It was observed from the tables and the charts that Davis et al. Model gave more consistent results, followed by Hopefield model then Altshuler and Kalaghan (A&K) Model. Furthermore, from the mean estimate in table 9 and the mean

deviation in table 10, the standard error of 0.285mm, 1.446mm and 2.899mm were respectively obtained for Davis et al. Model, Hopefield model and Altshuler and Kalaghan (A&K) Model.

Finally, from tables 11, 12, 13, the F-test showed that the differences in the performance of the standard tropospheric Models at each station are not statistically significant at 5% significance level.

5. Conclusions and Recommendations

5.1. Conclusions

Total zenith delays and gradient parameters can be estimated with the present GPS data processing. The zenith hydrostatic delay can be accurately inferred from precise measurements of atmospheric parameters. The magnitude of the estimated hydrostatic delay at a particular station depends on the hydrostatic delay model used and the time of observation. Based on the F-test performed, all the Models, i.e. Saastamoinen Model, Saastamoinen Model (Ground Meteorological Data), Davis et al. Model, Altshuler and Kalaghan (A&K) Model and Hopfield Model, generally produced results that are not statistically different. But comparatively, the Davis et al. Model with a standard error of about 0.3mm gave a better performance close to the adopted standard model, i.e. Saastamoinen Model. However, a standard deviation of about 1.4mm and 2.9mm for Hopefield and Altshuler and Kalaghan (A&K) Models respectively corroborate with the statistical test above. It could therefore, be concluded that either of the five models evaluated in this study can perform well in the study area, nevertheless, the choice of Saastamoinen Model, Saastamoinen Model (Ground Meteorological Data) and Davis et al. Model will be more preferable.

5.2. Recommendations

The following recommendations are made based on the research findings:

1. The best time for GPS observations with least tropospheric effect are between 2p.m and 6p.m. Also, observations at evening between 6p.m and 9p.m can be made as the tropospheric effect is not high during those times. However, observations at periods when the sun is said to be at its peak (11a.m to 1p.m) should be avoided.

2. Further researches like seasonal variations of tropospheric delay, the use of Continuously Observing Reference Stations (CORS) to investigate tropospheric impact, etc, should be encouraged for broader and better understanding of tropospheric effects.

REFERENCES

[1] Bevis, M., S. Businger, S. Chiswell, T.A. Herring, R.A. Anthes, C. Rocken and R. Ware (1994): GPS Meteorology: Mapping Zenith Wet Delays Onto Precipitable Water, Journal of Applied Meteorology, Vol. 33, pp. 379-386.

[2] Chao, C.C. (1972): A Model for Tropospheric Calibration from Daily Surface and Radiosonde, Balloon Measurement, Jet Propulsion Laboratory, Pasadena, California, Technical Memorandum 391-350, pp. 16.

[3] Davis, J.L., T.A. Herring, I.I. Shapiro, A.E.E. Rogers and G. Elgered (1985): Geodesy by Radio Interferometry: Effects of Atmospheric Modelling on Estimates of Baseline Length, Radio Science, Vol., 20, No. 6, pp. 1593-1607.

[4] Essen, L. and K.D. Froome (1951): The Refractive Indices and Dielectric Constants of Air and Its Principal Constituents at 24, 000 Mc/s. Proceedings of the Royal Society B, Vol. 64, pp. 862-875.

[5] Encyclopaedia Britannica (2009): Student and Home Edition.

[6] "Global Positioning System"(2010). www.gps.gov

[7] Hopfield, H.S. (1969): Two Quartic Troposheric Refractivity Profile for Correcting Satellite Data, Journal of Geophysical Research, Vol.74, No. 18, pp. 4487-4499.

[8] Hopfield, H.S. (1971): Tropospheric Effect on Electromagnetically Measured Range: Prediction from Surface Weather Data, Radio Science, Vol. 6, No. 3, pp. 357-367.

[9] Janes, H.W., R.B. Langley and S.B. Newby (1991): Analysis of Tropospheric Delay Prediction Models: Comparisons with Ray Tracing and Implications for GPS Relative Positioning, Bulletin Geodesique, Vol. 65, No. 3, pp. 151-161.

[10] Kaplan, E. D. and Hegarty, C.J. (2006): Understanding GPS; Principles and Applications, 2nd edition. Artech House, Inc.

[11] Lachapelle, G. (2001): Advanced GPS Theory and Applications, ENGO 625 Course Lecture Notes, University of Calgary, Calgary, Canada.

[12] Marini, J.W. (1972): Correction of Satellite Tracking Data for an Arbitrary Tropospheric Profile, Radio Science, Vol. 7, No. 2, pp. 223-231.

[13] Saastamoinen, J. (1972): Atmospheric Correction for Troposphere and Stratosphere in Radio Ranging Of Satellites, Geophysical Monograph, 15, American Geophysical Union, Washington, D.C., pp. 247-252.

[14] Saastamoinen, J. (1973): Contribution of the Theory of Atmospheric Refraction, Bulletin of Geodesique, No. 105, pp. 279-298, No. 106, pp. 383-397, No. 107, pp. 13-34.

[15] Satirapod, C., Chalermwattanachai, P. (2004): Impact of Different Tropospheric Models on GPS Baseline Accuracy: Case study in Thailand. A paper presented at the 2004 International Symposium on GNSS/GPS.

[16] Skone, S., M. El-Gizawy and S. M. Shrestha (2001): "Limitation In GPS Positioning Accuracies And Receiver Tracking Performance During Solar Maximum", Proceeding of KIS, Banff, Canada.

[17] Smith, E.K. and S. Weintraub (1953): The Constants in the Equation for Atmospheric Refractive Index at Radio Frequencies. Proceedings of I.R.E., Vol. 4, pp. 1035-1037.

[18] Spilker, J. J. (1996): Global Positioning System: Theory and Applications; "Tropospheric Effects on GPS", Chapter 13, Volume I, The American Institute of Aeronautics and Astronautics, Inc., Washington, D.C.

[19] Sudhir M. S. (2003): Investigations into the Estimation of Tropospheric Delay and Wet Refractivity Using GPS Measurements, Unpublished Master's Thesis, Geomatics Engineering Department, University of Calgary, Alberta, Canada.

[20] Thayer, G.D. (1974): An Improved Equation for the Radio Refractive Index of Air, Radio Science, Vol. 9, No. 10, pp. 803-807.